

High Temperature Thermal Expansion and Elastic Modulus of Steels Used in Mill Rolls

Alexander Laptev, Bernd Baufeld, Akhilesh Kumar Swarnakar, Stanislav Zakharchuk, and Omer van der Biest

(Submitted April 2, 2010; in revised form March 9, 2011)

The high temperature thermal expansion coefficient (TEC) and elastic modulus of five steels used in mill rolls production were investigated by dilatometer and impulse excitation techniques (IET). The measurements were provided at heating from room temperature till temperatures of about 1000 °C and subsequent cooling. The obtained data were attributed to the properties of predominating phases (austenite, martensite, pearlite, and bainite). The TEC and elastic modulus of corresponding phases were similar for all investigated steels despite the difference in their chemical composition. The steels with a chromium content of 2.95 wt.% and more show enhanced ability to quench hardening. This is an important prerequisite for production of high quality mill rolls.

Keywords elastic modulus, microstructure, mill rolls, thermal expansion

1. Introduction

Manufacturing of mill rolls is an important branch of modern metallurgy. The quality of rolls determines the efficiency of metal production. Particularly, the mill rolls should possess a hard surface layer with a thickness of about 50 mm. In the most cases, it is provided by quenching. Quenching of mill rolls is not a simple process because of the large size of the parts. For instance, Novo-Kramatorsk Machine Building Plant (NKMZ) in Ukraine produces rolls with the weight of up to 150 tons (Ref 1). For hardening of large rolls spray quenching by jets of water, air, or their mixture is commonly used. Due to intensive surface cooling, large temperature gradients arise within the bulk leading to thermal stresses. The thermal stresses cause elastic, plastic, and creep strains and can influence the phase transformation at quenching. The complex interplay of thermal, mechanical, and metallurgical fields results into residual stresses in the rolls. These stresses are often the reason for cracks and fracture. It is rather impossible to predict even qualitatively the level and distribution of residual stresses based only on

intuition or previous experience. This problem becomes more challenging taking into account the individual character of large rolls manufacturing. Finite element computer simulation of roll quenching is a good approach for predicting such residual stresses.

Several finite element models of quenching are described in the literature (Ref 2-4). The models were used for the prediction of temperature, stress and phase distribution, most often in relatively small parts made from carbon steel. Much less modeling work is dedicated to the quenching of large industrial parts such as turbine rotors, engine shafts, or mill rolls (Ref 5). One reason for that is the lack of input information on properties of alloyed steels used for their manufacturing. The aim of the present article is to reduce the gap between theory and practice by experimental investigation of elastic modulus and thermal expansion of some typical steels used for mill rolls. These data are necessary for the calculation of thermal stresses and strains at quenching. Since the temperature at quenching may be subject to a variation between 1000 and 20 °C, the dependences of thermal expansion coefficient (TEC) and elastic modulus on quenching temperature were determined in this range.

Iron in steels has body-centered cubic (bcc) and face-centered cubic (fcc) crystal structures. Body-centered cubic structure of iron is inherent for ferrite, pearlite, and bainite. Face-centered cubic structure of iron is known as austenite. Iron can also form a body-centered tetragonal structure of martensite due to supersaturating with carbon at quenching. The bond energy dependencies on interatomic spacing in such structures are different. This is a reason for TEC and elastic modulus dependences on the microstructure of steels. Therefore, the obtained data were also associated with the phase constitutions of steels in temperature range of their predominance.

The thermal expansion was studied by dilatometry and the elastic modulus by impulse excitation technique (IET). The microstructure and the phases were examined by light microscopy, scanning electron microscopy (SEM), and x-ray diffraction (XRD). The identification of the phases was supported by microhardness measurements.

Alexander Laptev, Bernd Baufeld, Akhilesh Kumar Swarnakar, and Omer van der Biest, Department of Metallurgy and Materials Engineering, Katholieke Universiteit Leuven, Kasteelpark Arenberg 44, B-3001 Heverlee, Belgium; Alexander Laptev, Department of Materials Science and Engineering, Donbass State Engineering Academy, Shkadinova 72, UA-84313 Kramatorsk, Ukraine; and Stanislav Zakharchuk, Laboratory of Mill Rolls, Novo-Kramatorsk Machine Building Plant (NKMZ), UA-84305 Kramatorsk, Ukraine. Contact e-mail: laptev@dgma.donetsk.ua.

2. Experimental Setup

2.1 Steels Compositions

Five different steel grades used at mill rolls production were delivered from NKMZ. The chemical composition of steels was determined by x-ray fluorescence spectrometer (Philips PW 2400, Netherlands). The results are summarized in Table 1. The specimens were marked corresponding to their carbon content. The decrease in carbon content is accompanied by an increase in chromium level. The microstructure and hardness of as received steels are described in section 3.

2.2 Dilatometry, IET

The thermal expansion studies were performed in Ar up to 1000 °C using a dilatometer (NETZSCH DIL 402 C/7, Selb, Germany). The specimens were 10 mm in height and 10 mm in diameter. The heating and cooling rates were maintained at 5 °C/min to ensure a homogeneous temperature distribution within the samples. Much larger cooling rates at quenching can be expected. Nevertheless, this fact has no influence on TEC of particular phase as well as on elastic modulus.

The dependence of elastic moduli on temperature has been studied by impulse excitation technique (IET), which has been described in detail elsewhere (Ref 6, 7). A light impact excites a suspended specimen into the resonance frequency, which, in the present case, is measured by a microphone. The elastic modulus then can be calculated, since the square of the resonance frequency is proportional to the elastic modulus. The repeatability coefficient for IET at the 95% confidence level within laboratory is estimated as about 1% (Ref 8). The high temperature IET tests were performed inside a graphite furnace HTVP-1750C° in Ar atmosphere, using carbon wires for suspension of the specimens, and analyzed by the RFDA software (IMCE, Genk, Belgium) between room temperature and 920 °C, applying a heating and cooling rate of 3 °C/min. The slow heating and cooling has provided a homogeneous temperature within samples. For IET measurements, steel specimens were cut by diamond saw into a rectangular

geometry of roughly 50 × 3 × 2 mm³ and polished before measurement to remove surface contaminations.

2.3 Microscopy, XRD, and Hardness

The microstructure was examined on cross sections of test specimens before and after dilatometry by using light microscopy and SEM (XL30-FEG, FEI, Eindhoven, Netherlands). The Nital solution with 3% concentration of nitric acid was used for etching. Phase analysis was performed by XRD (3003-TT, Seifert, Ahrensburg, Germany) from 2 θ = 20° to 120° on specimens before and after dilatometry. The hardness has been investigated applying a Vickers microindenter (Durimet 2, Leitz, Wetzlar, Germany) with a 100 g load. For every specimen, 20 indentations were performed 0.5 mm apart. By this, an average was achieved disregarding possible microstructural inhomogeneity.

3. Results

3.1 Microstructure

Depending on the chemical composition different microstructures before and after dilatometry were observed for different steels (Table 2). Figure 1 shows examples of microstructures observed by light microscopy and Fig. 2 shows microstructures observed by SEM. Steel 50 has in the as-received state a two-phase structure of bainite grains decorated by the pearlite phase (Fig. 1a, 2a). Steels 65 and 75 show as received a globular structure (Fig. 2c, g) and steels 70 and 90 exhibit a lamellar pearlite structure (Fig. 2e, i). After the dilatometry, steels 50, 65, and 70, i.e., chromium rich steels, exhibit structures with decorated grain boundaries (Fig. 1b-d, 2b, d, f). The decorating phase of steel 50 is attributed to bainite and of steels 65 and 70 to pearlite. The phase in the grains of steel 50 after dilatometry can be assigned to martensite (Fig. 1b, 2b) and in the grains of steel 65 to bainite (Fig. 1c, 2d). For steel 70 two different phases can be observed for the grains (Fig. 1d, 2f). One type of these two phases gives a speckled

Table 1 Alloying elements in steels (wt.%)

Steel	C(a)	Mn	Si	Cr	Ni	Mo	V
50	0.43-0.50	0.611 ± 0.030	0.929 ± 0.046	4.31 ± 0.10	0.449 ± 0.047	0.501 ± 0.054	0.0546 ± 0.007
65	0.65-0.70	0.553 ± 0.028	0.706 ± 0.035	3.61 ± 0.09	0.091 ± 0.043	0.750 ± 0.060	0.256 ± 0.013
70	0.65-0.75	1.16 ± 0.050	0.601 ± 0.030	2.95 ± 0.08	0.115 ± 0.045	0.681 ± 0.066	0.257 ± 0.013
75	0.70-0.80	0.275 ± 0.016	0.442 ± 0.022	1.47 ± 0.06	0.096 ± 0.048	0.104 ± 0.056	0.055 ± 0.007
90	0.85-0.95	0.393 ± 0.024	0.555 ± 0.028	1.66 ± 0.06	0.255 ± 0.077	0.088 ± 0.085	0.179 ± 0.012

(a) Supplier data

Table 2 Microstructure and hardness of steels as received and after dilatometry

Steel	50	65	70	75	90
Microstructure					
As received	Bainite and pearlite	Globular pearlite	Lamellar pearlite	Globular pearlite	Lamellar pearlite
After dilatometry	Martensite and bainite	Bainite and pearlite	Martensite bainite and pearlite	Lamellar pearlite	Lamellar pearlite
Hardness (HV)					
As received	370 ± 36	221 ± 4	335 ± 22	180 ± 6	329 ± 12
After dilatometry	791 ± 22	478 ± 20	742 ± 48	357 ± 11	332 ± 10

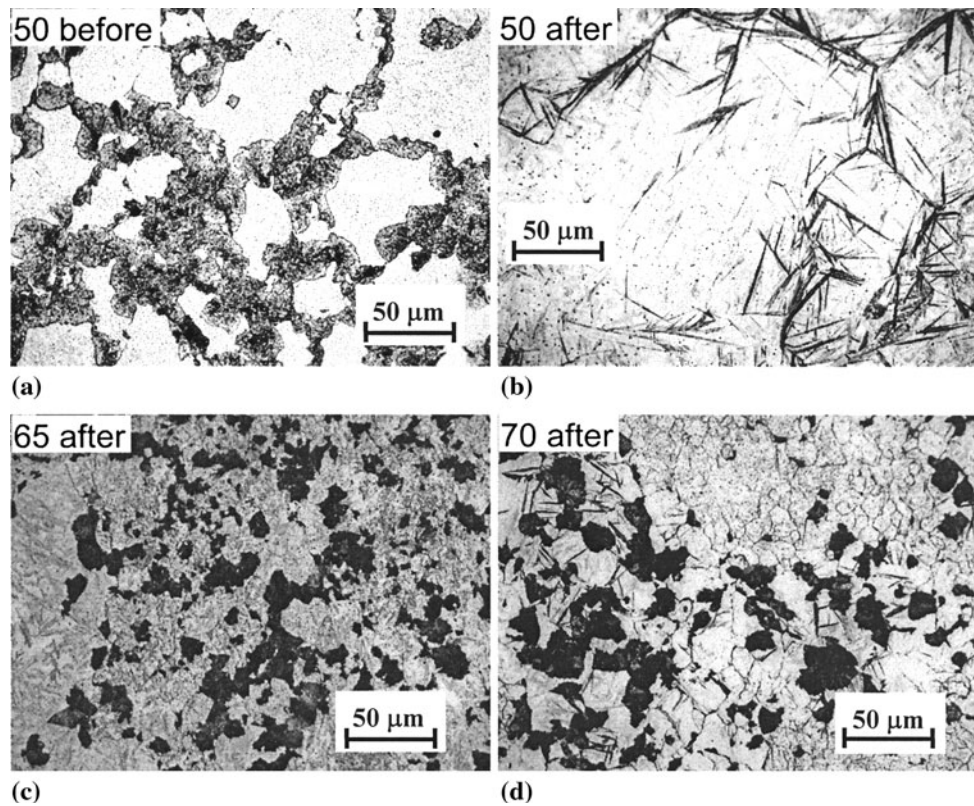


Fig. 1 Optical micrographs of steel specimens, exhibiting a microstructure with decorated grain boundaries before and after dilatometry. The phases of the grains are bainite (a, c), martensite (b), or their mixture (d)

contrast assigned to bainite, the other exhibits spikes typical for martensite. The amount of the decorating phase varies from the minor amount for steel 50 to the highest one for steel 65. Steels 75 and 90 display a lamellar pearlite microstructure after dilatometry (Fig. 2h, j).

For all investigated alloys before and after dilatometry, the strongest XRD reflection pattern derives from α ferrite. In addition, reflections from retained γ austenite exist for steels 50 and 65 after and for steel 50 before dilatometry (Fig. 3). The amounts of austenite are roughly 5 and 7% for steel 50 before and after dilatometry, and roughly 10% for steel 65 after dilatometry. Steel 70 exhibits a weak reflection at 44° before dilatometry and a rather broad and asymmetric α peak after dilatometry (Fig. 3). Possibly, this shoulder can be interpreted as a nonresolved peak splitting from α austenite and α' martensite. To summarize, the steels with globular or lamellar pearlite microstructure show only α diffraction patterns, while other steels give indications for retained austenite or martensite. These microstructure investigations have been used to support the interpretation of phase changes observed during dilatometer and IET experiments.

3.2 Microhardness

Microhardness measurements were used as a supporting tool for the phase identification. The results of the measurements are shown in Table 2. The hardness is closely related with the microstructure. The globular pearlite exhibits the lowest hardness of about 200 HV, while the lamellar pearlite, both before and after dilatometry, has a hardness in the range of 330 HV. The highest average hardness is observed for the steels

with multiphase microstructure. More detailed investigations reveal high hardness in the center of the grains, and much lower hardness of the decorating phase. For instance, for steel 50 in the as-received state the corresponding average values were 465 HV for the bainite grains and 330 HV for the decorating pearlite phase. The two different hardness regimes of the structure components are the reason for the large variation observed for steel 50 before, and for steel 70 after dilatometry. The variation for steel 50 after dilatometry is small due to the minor amount of the decorating phase. In this case mainly the grains were measured.

3.3 Dilatometry

The dilatation curves of the five different steels generally exhibit thermal expansion during heating (Fig. 4). In addition, all steels show a significant contraction at temperatures about 800°C , attributed to pearlite to austenite transition. This transformation appears at higher temperatures for steel 50 than for the other steels. During a subsequent dilatometry cycle of this specimen, the dilatation curve exhibits a slight bend at 400°C at heating, which is interpreted as the decomposition of martensite to ferrite and cementite (Fig. 4b).

The cooling curves are more complex and differ for the different steels, exhibiting between one to three known transitions, namely an austenite to pearlite transition at high temperature (T_{HT}), an austenite to bainite transition at intermediate temperature (T_{IT}), and an austenite to martensite transition at low temperature (T_{LT}). Steels 75 and 90 both show only austenite to pearlite transitions at temperatures about 680°C ,

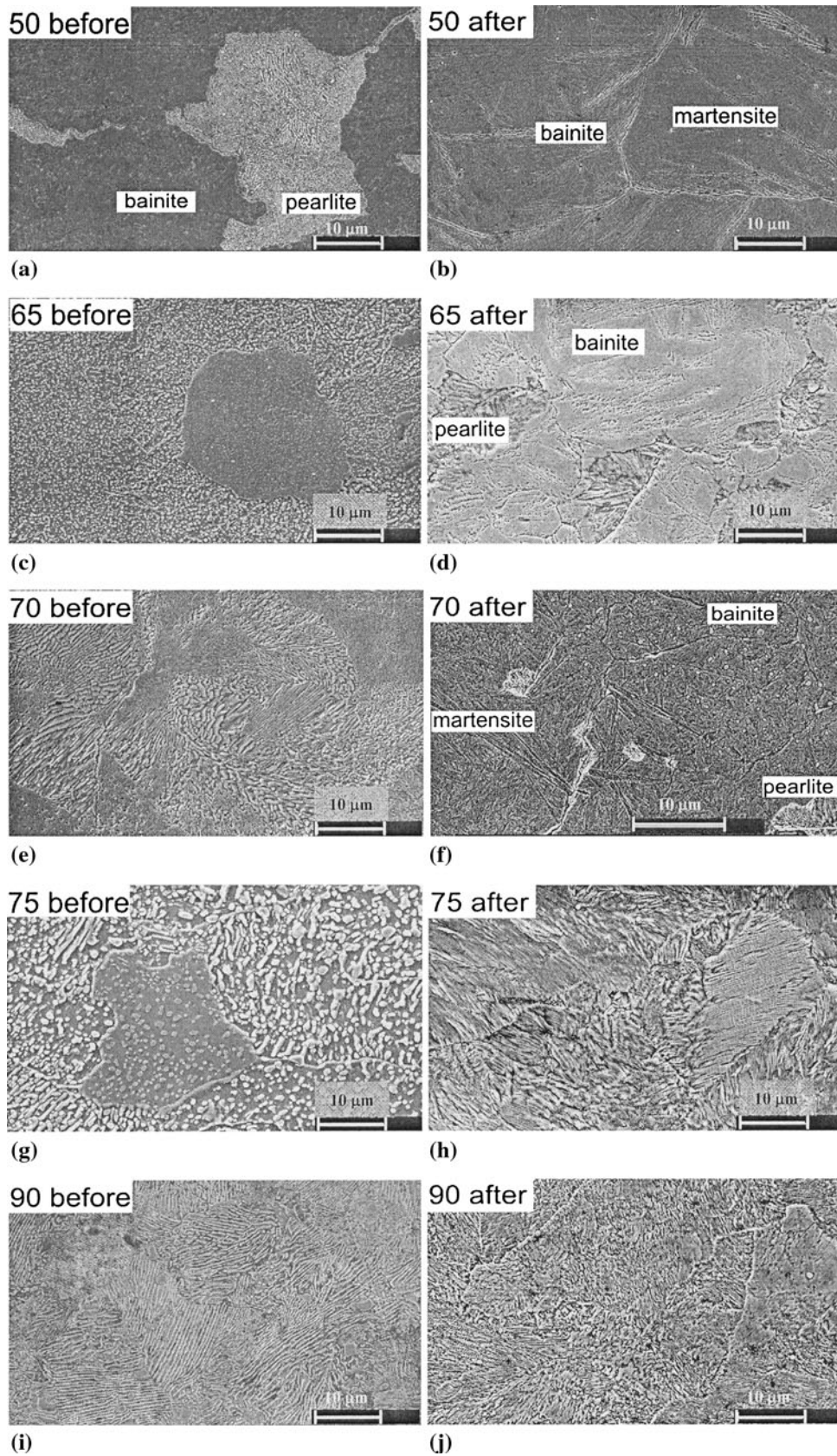


Fig. 2 Scanning electron micrographs of the steel specimens before and after dilatometry

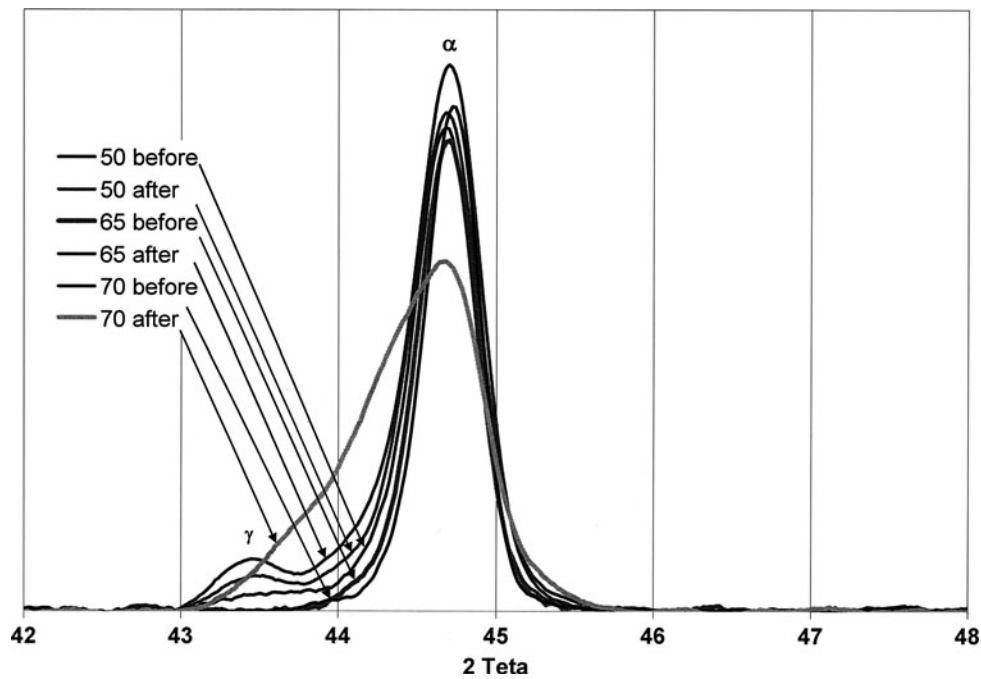


Fig. 3 XRD patterns of the Cr rich specimens (Cr amount ≥ 2.95 wt.%) before and after dilatometry for $2\theta = 42^\circ\text{--}48^\circ$

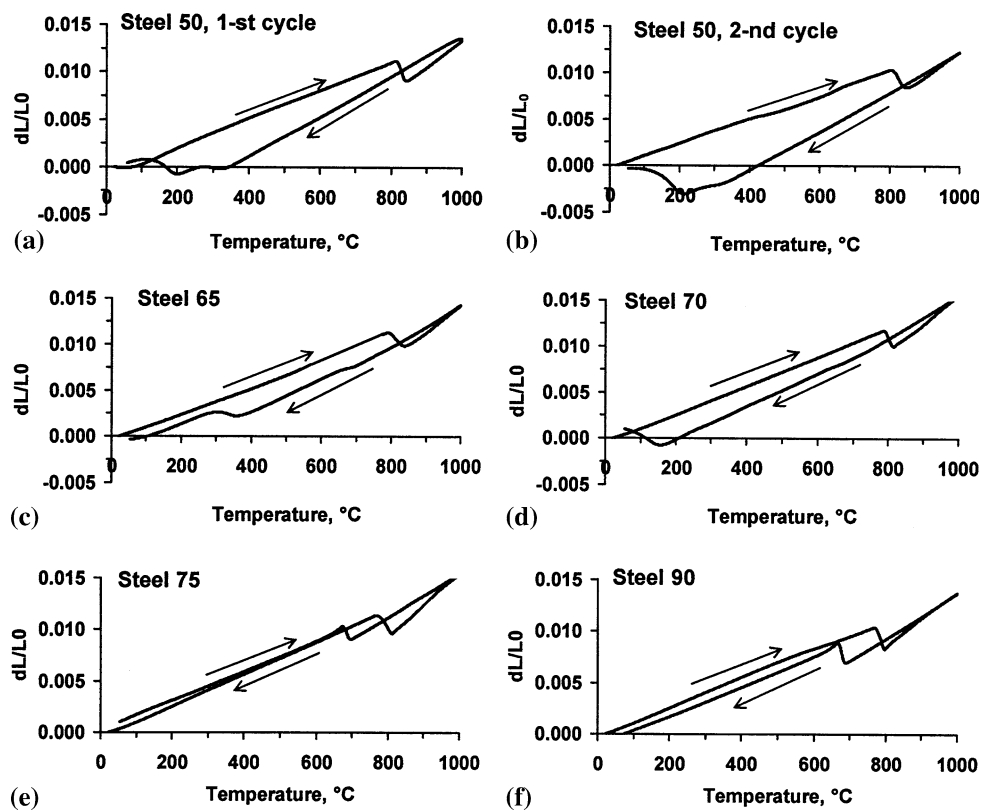


Fig. 4 Dilatometry curves of different steel specimens

where the expansion is comparable in amount with the contraction during heating. For steels 65 and 70 only weak and for steel 50 no clear indications for an austenite to pearlite transformation can be seen.

Steels 50, 65, and 70 also display an austenite to bainite transition during cooling about 300°C and steels 50 and 70 a martensitic transformation below 200°C . All transition temperatures are summarized in Table 3. The dilatometry results

are in good agreement with the microstructure observation discussed in section 3.1.

3.4 Impulse Excitation Technique

Figure 5 shows the dependence of the elastic modulus on temperature during heating and cooling for all five steels. In general, a decrease of the elastic modulus with increasing temperature is observed. Similar to the dilatometry, different step-like changes in different temperature regimes occur. These changes are attributed to the same transitions as observed during dilatometry, and their transition temperatures are also summarized in Table 3. The slight difference in the corresponding transition temperatures determined from dilatometry and IET tests relates to the different heating and cooling rates of these experiments.

During heating all steels exhibit a pearlite to austenite (bcc to fcc) transition at about 800 °C, leading to a step-like decrease of the elastic modulus. Similar to the case of dilatometry, the pearlite to austenite transition of steel 50 occurs at higher temperatures than for the other specimens. During cooling, in the case of steels 90 and 75, at temperatures about 100 °C lower than during heating, the austenite totally reverses to pearlite, closing the heating/cooling curves. This leads to similar values of the elastic modulus before and after testing. For the other steels, the austenite to pearlite transition at cooling is much weaker or hardly noticeable and not completed. Therefore, at corresponding temperatures the elastic modulus is lower during cooling than during heating. The change of the elastic modulus due to bainitic transformation T_{IT} is observed for steels 50, 65, and 70. Indications for the influence of martensitic transition on

Table 3 Transition temperatures during dilatometry and IET experiments (°C)

Experimental technique	Phase transition	Steel				
		50	65	70	75	90
Dilatometry						
Heating	Pearlite → austenite	809-870	783-876	783-823	765-820	767-802
Cooling	Austenite → pearlite		707-623	652-n.a.	700-665	698-657
	Austenite → bainite	352-215	390-n.a.	302-n.a.		
	Austenite → martensite	215-65		180-n.a.		
IET						
Heating	Pearlite → austenite	695-780	714-797	725-792	735-775	725-771
Cooling	Austenite → pearlite	686-632	683-623	666-607	710-678	710-680
	Austenite → bainite	416-287	406-279	415-275		

n.a., not allocable

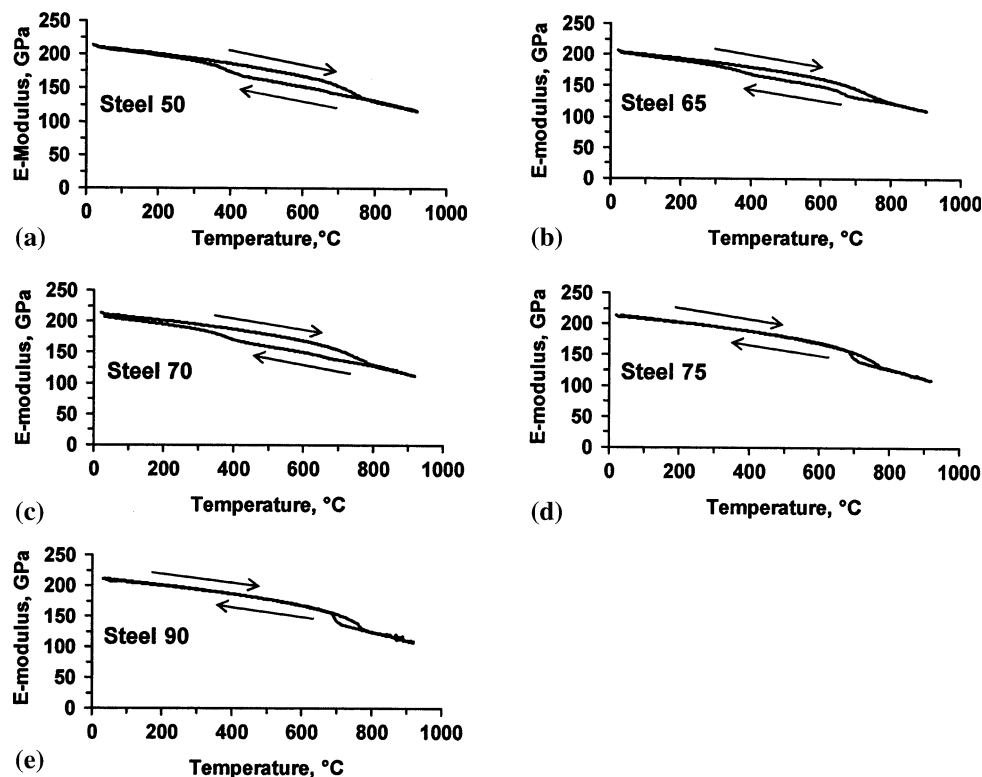


Fig. 5 Temperature dependencies of the elastic moduli for different steel specimens

elastic modulus cannot be reported in the case of IET experiments.

4. Discussion

4.1 Phase Transitions

The analysis of phase transitions allows the estimation of a temperature range where only one phase exists or predominates. The phase transitions are dependent on the chemical composition of the steel and the heating/cooling rate. Therefore, they may have some peculiarities at testing of different steels by dilatometry (5 °C/min) and by IET (3 °C/min) explaining the shift of transition temperatures between these two different experiments.

The initial pearlite structure of steels 75 and 90, respectively, was retained at heating in the dilatometer until the temperature of austenite formation was reached. The complete austenite to lamellar pearlite reverse transformation was observed at cooling (Fig. 4e, f). Thus, the temperature interval where only pearlite or austenite exists can be easily defined at heating and cooling of these two steels by dilatometry. The TEC values observed in this temperature interval can be related to the corresponding phases.

The initial structures of steels 65 and 70 are globular and lamellar pearlite, respectively. These structures retain during heating at dilatometry tests up to the temperature of austenitic formation. Despite the fact that the initial structure of steel 50 consists of pearlite and bainite, no evidence of bainite decomposition can be seen on dilatometer curve at heating until the temperature of austenitic formation. This can be explained by identical thermal expansion of pearlite and bainite (see also section 4.2). Therefore, in Table 4 TEC of pearlite and bainite mixture was attributed to pearlite. Thus, the TEC of these three steels in pearlite and austenite state can be determined at heating.

The phase transition at cooling of steels 50, 65, and 70 is more complicated comparing to the steels 75 and 90. This difference is related to the larger amount of alloying elements, particularly chromium. Chromium causes the shift of the contours in the Time-Temperature-Transformation (TTT) diagram to the right. Correspondingly, it decreases the cooling rates at which bainitic and martensitic transformations occur (Ref 9). The austenite was fully stable at cooling before the pearlite formation— T_{HT} began. In the case of steel 50, the transformation T_{HT} was not observed. The transformation of austenite for this steel starts at a lower, intermediate temperature T_{IT} resulting some amount of bainite. Thus, the TEC of austenite can be determined in the region between maximal

temperature and the temperature of T_{HT} for steels 65 and 70 and in the region between maximal temperature and the temperature of T_{IT} for steel 50. The austenite to pearlite transformation is not completed in all cases. Therefore, the mixed structure of austenite and pearlite is expected in the temperature range between T_{HT} and T_{IT} impeding the determination of a relation between measured thermal expansion and the respective phases. The transition of austenite to bainite was observed for steels 50, 65, and 70, followed by the martensitic transformation. The steel 65 shows the pronounced austenite to bainite transformation and only a weak martensitic transformation. Therefore, the resulting structure consists mainly of bainite and pearlite (Fig. 1c and 2d). On the other hand, steels 50 and 70 show in the case of dilatometry a moderate bainitic and a pronounced martensitic transformation. Therefore, the microstructure of steel 70 consists of pearlite, bainite, and martensite after dilatometry (Fig. 1d and 2f). The microstructure of steel 50 includes predominantly martensite and some amount of bainite (Fig. 1b and 2b). This statement is supported by hardness measurements (see Table 2). The steel 50 has the largest hardness due to the largest content of martensite.

Thus, during cooling steels 65, 70 after the transformation T_{HT} and steel 50 after the transformation T_{IT} , have multiphase compositions. This makes it impossible to relate the measured thermal expansion in these temperature intervals to a certain phase. To estimate the TEC of martensite, the specimen of steel 50 was tested in the dilatometer twice. Before the second dilatometer run the specimen had a predominantly martensitic structure (Fig. 1b, 2b). The martensite was retained up to temperature about 400 °C. Therefore, the TEC of martensite could be determined in this temperature range.

The IET results can be analyzed in analogy to the dilatometry. Temperature dependencies of elastic modulus for steels 75 and 90 show the closed loops of pearlite and austenite transformation and clear temperature ranges of their existence (Fig. 5d, e). Thus, the elastic modulus can be related to pearlite and austenite at IET experiments for these two steels. Steels 50, 65, and 70 show the pronounced pearlite to austenite transition at heating (Fig. 5a-c). Therefore, the elastic modulus of pearlite and austenite can be determined during heating. The temperature at the beginning of T_{HT} and the temperature range of incomplete austenite to pearlite transition can be seen in cooling curves for these steels (Fig. 5a-c). Finally, a pronounced transformation of austenite to bainite is observed. Thus, the elastic modulus can be related to austenite in the interval between maximal temperature and the temperature at T_{HT} and to pearlite and bainite mixture at temperatures after T_{IT} .

4.2 Thermal Expansion

The dependence of thermal expansion on temperature was observed to be nearly linear in regions where one phase is predominant. This leads to constant values of TEC for certain phases. It is known that the TEC is influenced by the chemical composition of an alloy. Particularly, the increase of chromium content in the iron matrix over 5% leads to a noticeable decrease of the thermal expansion (Ref 10). The influence of the combination of alloying elements is not systematically documented.

The TEC of pearlite or bainite and pearlite mixture was determined for all five steels at heating and for steels 75 and 90 at cooling. The results are presented in Table 4. The largest difference of TEC for two steels at heating is 5.3% in respect to

Table 4 TEC of pearlite and austenite determined for different steels ($10^{-6}/^{\circ}\text{C}$)

Steel	50	65	70	75	90	Average
Pearlite						
Heating	14.8	15.0	15.6	15.5	14.8	15.1
Cooling	14.3	14.3	14.3
Austenite						
Heating	28.2	29.4	30.7	31.5	26.3	29.2
Cooling	21.2	22.0	23.0	21.2	21.7	21.8

Table 5 Elastic modulus of pearlite determined for different steels (GPa)

Temperature, °C	Steel					Average
	50	65	70	75	90	
25	212	205	212	213	211	211
200	201	194	202	203	201	200
400	185	180	187	189	187	186
600	167	161	169	169	167	167

the mean value of $15.1 \cdot 10^{-6}/^{\circ}\text{C}$. The last value is in very good agreement with the data for pearlite and ferrite in the case of C60 steel (0.57-0.6 C, 0.6-0.9 Mn, ≤ 0.4 Si, ≤ 0.4 Cr, ≤ 0.4 Ni, ≤ 0.1 Mo, wt.%) (Ref 2). The TEC of pearlite during cooling is the same for steels 75 and 90. The corresponding value of $14.3 \cdot 10^{-6}/^{\circ}\text{C}$ is by 5.3% lower than during heating. The TEC of austenite was determined for all steels during heating and cooling. The results are summarized in the Table 4. The largest difference of TEC for two steels during heating is 11.3% in respect to the average value of $29.2 \cdot 10^{-6}/^{\circ}\text{C}$. The TEC during cooling is much less than during heating. The variance is in the range of 8.3% relative to the average value of $21.8 \cdot 10^{-6}/^{\circ}\text{C}$. The last number is in a very good agreement with the data for C60 steel (Ref 2). The TEC of pearlite and bainite mixture was also defined during cooling of steel 65, which shows completed bainitic transformation below 279 °C (Fig. 4c). The obtained value of $15.1 \cdot 10^{-6}/^{\circ}\text{C}$ is the same as for pearlite during heating. Therefore, we can conclude that pearlite and bainite have a similar TEC. The TEC of martensite was defined during second heating of steel 50 between room temperature and 400 °C. The obtained value of $1.35 \cdot 10^{-6}/^{\circ}\text{C}$ is close to the data known for steel C60 (Ref 2).

In conclusion, the chemical composition of the investigated steels does not have a large influence on the TEC of pearlite and austenite (Table 4). The TEC of these phases during heating is higher than during cooling especially for austenite. The reason for this discrepancy is not understood. The obtained values of TEC can be used for modeling of thermal stresses at quenching of the mill rolls produced from these steels.

4.3 Elastic Modulus

As expected, the elastic modulus of all steels varies with temperature and phase (Fig. 5). The temperature dependence of elastic modulus during heating and cooling of steels 75 and 90 is fully reversible due to complete pearlite to austenite and austenite to pearlite transformation. The values of the elastic modulus for these steels in pearlite and austenite regions are presented in Table 5 and 6. For the other three steels, the elastic moduli at high temperatures can also be attributed to austenite and are also shown in Table 6. Since, during cooling of steel 50 the austenite remains stable up to temperatures about 400 °C, the elastic modulus of austenite can be determined over a wider temperature range. For steels 65 and 70, the temperature dependence of elastic modulus for pearlite was also determined during heating. The results for pearlite are summarized in Table 5. The elastic modulus of pearlite and bainite mixture was estimated at cooling for the steels 50, 65, and 70. The values in the corresponding temperature regions are slightly lower than the ones for pearlite. This difference can be attributed to the presence of the retained austenite. For engineering calculations,

Table 6 Elastic modulus of austenite determined for different steels (GPa)

Temperature, °C	Steel					Average
	50	65	70	75	90	
400	170	170
600	152	152
800	130	122	130	126	123	126
900	119	110	114	111	110	113

the elastic modulus of pearlite and bainite and pearlite mixture can be regarded as identical.

In conclusion, the elastic moduli of pearlite and austenite do not show any significant dependence on chemical compositions for investigated steels. The obtained values are in a very good agreement with the data for steel C60 (Ref 2).

5. Conclusions

The thermal dependence of TEC and elastic modulus during heating and cooling has been investigated in five different steel compositions and the changes in TEC and elastic moduli have been related to the associated phase transformations. The major findings of the study are following:

- The two steels containing <2 wt.% chromium, show only pearlite to austenite transformation during heating and fully reverse transformation during cooling at 5 °C. The other three steels, containing 2.95 wt.% and more chromium and an increased amount of manganese and molybdenum, show during cooling at 5 °C the bainitic transformation in addition. Steels 50 and 70 display at cooling also a pronounced martensitic transformation. These two steels should have the lowest critical cooling rate leading to a thicker hard martensitic layer at the same quenching condition. This is an important prerequisite for production of high quality mill rolls. It is necessary to underline that observed transformation temperatures and resulting microstructures are relevant only for discussed steels with certain compositions after heating and cooling with specific rate.
- Despite the difference in both chemical composition and their peculiarities of phase transition, all five steels have similar TEC in the pearlite as well as in austenite state. During cooling, the values of TEC for pearlite are only slightly (about 6%) lower than the values during heating. However, the TEC of austenite during heating far exceeds the values during cooling. The average difference is about 34%. The reason is not understood. The average values of TEC of pearlite during heating and of austenite during cooling are $1.51 \cdot 10^{-6}/^{\circ}\text{C}$, respectively, $2.18 \cdot 10^{-6}/^{\circ}\text{C}$. These values are in a good agreement with literature data for high carbon steel (Ref 2). The TEC of martensite of $1.35 \cdot 10^{-6}/^{\circ}\text{C}$ determined during heating also well corresponds with literature data for high carbon steel (Ref 2).
- The temperature dependences of the elastic modulus of pearlite and austenite are similar for all investigated steels. No difference in elastic modulus was observed during heating and cooling if the phase constitution was the same. The elastic modulus of austenite is 9-10% lower

than of pearlite at temperatures of 400 and 600 °C. The elastic modulus of bainite and pearlite mixture was found to be identical to the modulus of pearlite. The obtained temperature dependencies of the elastic modulus closely agree with the literature data for high carbon steel.

- The gained information on high temperature thermal expansion and elastic modulus of steels can be used for the modeling and development of mill rolls quenching.

Acknowledgments

Alexander Laptev thanks the Ministry for Education and Science of Ukraine for financial support of this work by project no. 0107U001301 and the K.U. Leuven Research Council for his research fellowship no. F/02/096.

References

1. Yu.N. Belobrov, I.G. Volchenkov, V.B. Shabanov, and O.V. Sviridov, Production of Rolling-Mills Rolls at the Novokramatorsk Machine Plant, *Metallurgist (N.Y., N.Y., U.S.)*, 2001, **45**(1–2), p 84–86
2. C.H. Gür and A.E. Tekkaya, Numerical Investigation of Non-homogeneous Plastic Deformation in Quenching Process, *Mater. Sci. Eng. A*, 2001, **319–321**, p 164–169
3. S.H. Kang and Y.T. Im, Thermo-Elasto-Plastic Finite Element Analysis of Quenching Process of Carbon Steel, *J. Mater. Process. Technol.*, 2007, **192–193**, p 381–390
4. H. Li, G. Zhao, S. Niu, and C. Huang, FEM Simulation of Quenching Process and Experimental Verification of Simulation Results, *Mater. Sci. Eng. A*, 2007, **452–453**, p 164–169
5. C.C. Liu, X.J. Xu, and Z. Liu, A FEM Modeling of Quenching and Tempering and Its Application in Industrial Engineering, *Finite Elem. Anal. Des.*, 2003, **39**(11), p 1053–1070
6. G. Roebben, B. Basu, J. Vleugels, J. Van Humbeeck, and O. Van der Biest, The Innovative Impulse Excitation Technique for High-Temperature Mechanical Spectroscopy, *J. Alloys Compd.*, 2000, **310**(1–2), p 284–287
7. G. Roebben, B. Bollen, A. Brebels, J. Van Humbeeck, and O. Van der Biest, Impulse Excitation Apparatus to Measure Resonant Frequencies, Elastic Moduli, and Internal Friction at Room and High Temperature, *Rev. Sci. Instrum.*, 1997, **68**(12), p 4511–4515
8. ASTM C 1259-08, “Standard Test Method for Dynamic Young’s Modulus, Shear Modulus, and Poisson’s Ratio for Advanced Ceramics by Impulse Excitation of Vibration,” ASTM, 2008
9. Yu.M. Lakhtin, V.P. Leonteva, *Материаловедение (Materials Science)*, Moscow, Mashinostroenie, 1972 (in Russian)
10. T. Malkow, U. Von der Crone, A.M. Laptev, T. Koppitz, U. Breuer, and W.J. Quadackers, Thermal Expansion Characteristics and Corrosion Behavior of Ferritic Steels for SOFC Interconnects, *Proceedings of the 5th International Symposium on Solid Oxide Fuel Cells*, Vol 97(40), U. Stimming, S.C. Singhal, H. Tagawa, and W. Lehnert, Eds., June 2–5, 1997 (Aachen), Electrochemical Society Inc., 1997, p 1244–1252